FEBS Letters 583 (2009) 1323–1326

FEBS Letters

journal homepage: www.FEBSLetters.org

Crystal structure of polysaccharide lyase family 20 endo-β-1,4-glucuronan lyase from the filamentous fungus *Trichoderma reesei*

Naotake Konno [a,1], Takuya Ishida [a,1], Kiyohiko Igarashi [a], Shinya Fushinobu [b,*], Naoto Habu [c], Masahiro Samejima [a], Akira Isogai [a]

[a] Department of Biomaterials, Graduate School of Agricultural and Life Sciences, The University of Tokyo, 1-1-1 Yayoi, Bunkyo-ku, Tokyo 113-8657, Japan
[b] Department of Biotechnology, Graduate School of Agricultural and Life Sciences, The University of Tokyo, 1-1-1 Yayoi, Bunkyo-ku, Tokyo 113-8657, Japan
[c] Department of Bioproductive Science, Utsunomiya University, 350 Mine-machi, Utsunomiya, Tochigi 321-8505, Japan

ARTICLE INFO

Article history:
Received 24 February 2009
Revised 11 March 2009
Accepted 16 March 2009
Available online 22 March 2009

Edited by Richard Cogdell

Keywords:
Cellouronate
Glucuronan
TEMPO oxidation
Polysaccharide lyase
β-Jelly roll fold
Trichoderma reesei

ABSTRACT

The crystal structure of endo-β-(1→4)-glucuronan lyase from *Trichoderma reesei* (TrGL) has been determined at 1.8 Å resolution as the first three-dimensional structure of polysaccharide lyase (PL) family 20. TrGL has a typical β-jelly roll fold, which is similar to glycoside hydrolase family 16 and PL7 enzymes. A calcium ion is bound to the site far from the cleft and appears to contribute to the stability. There are several completely conserved residues in the cleft. Possible catalytic residues are predicted based on structural comparison with PL7 alginate lyase A1–II′.

1. Introduction

Anionic polysaccharides, such as alginate, pectate/pectin, xanthan, and hyaluronan, are degraded by their corresponding lyases. Polysaccharide lyases (PLs) recognize uronic acid residues in polysaccharides and catalyze the β-elimination reaction with concomitant formation of a C4–C5 double bond within the uronic acid moiety at the non-reducing end. Currently, PLs are classified into 21 families based on their amino acid sequence similarities in the Carbohydrate-Active enZymes database (CAZy, http://www.cazy.org) [1]. Among them, three-dimensional structures of enzymes in PL1–11, 16, 18, 19, and 21 have been determined. Structural scaffolds of the catalytic domain of PLs are diverse and can be categorized into five groups; β-helix (PL1, 3, 6, 9, 16, and 19), α/α-barrel (PL2, 5, 8, 10, and 21), β-sandwich plus β-sheet (PL4), β-jelly roll (PL7 and 18), and β-propeller (PL11).

Polyglucuronate (glucuronan) is a minor polysaccharide compared with other polyuronates. But β-(1→4)-glucuronan structures are found in bacteria [2], fungi [3], and algae [4] as water-soluble polysaccharides. To date, glucuronan lyases (EC 4.2.2.14) have been identified in several organisms. A PL14 enzyme from chlorovirus cleaves β- or α-(1→4)-glucuronan in the cell wall of *Chlorella* strains [5]. *Sinorhizobium meliloti* mutant strain M5N1CS produces partially acetylated β-(1→4)-glucuronan and an endogenous glucuronan lyase [6]. The bacterial glucronan is also depolymerized by an *endo*-type lyase from a fungus, *Trichoderma* sp. GL2 [7]. Cellouronate, a pure β-(1→4)-glucuronan without any acetyl groups, is prepared from regenerated cellulose by 2,2,6,6-tetramethylpiperidine-1-oxyl radical-mediated oxidation. Recently, we isolated a bacterial strain, *Brevundimonas* sp. SH203, that can degrade cellouronate and purified two β-(1→4)-glucuronan lyases, which catalyze *endo*- and *exo*-type depolymerization of cellouronate, respectively [8,9].

In the previous report, we cloned the gene encoding an *endo*-β-(1→4)-glucuronan lyase (TrGL) from the filamentous fungus *Trichoderma reesei* (*Hypocrea jecorina*) NBRC 31329 [10]. The amino acid sequence showed no similarity to those of other known PLs, and the enzyme has been classified into a novel family, PL20. TrGL is highly specific for β-(1→4)-glucuronan, and its activity and

Abbreviations: PL, polysaccharide lyase; CAZy, Carbohydrate-Active enZymes; TrGL, *Trichoderma reesei* glucuronan lyase; RMSD, root mean square deviation

* Corresponding author. Fax: +81 3 5841 5151.
E-mail address: asfushi@mail.ecc.u-tokyo.ac.jp (S. Fushinobu).

[1] These authors contributed equally to this work.

0014-5793/$36.00
doi:10.1016/j.febslet.2009.03.034

thermostability increased in the presence of Ca^{2+} [10]. Here we report the crystal structure of TrGL as the first three-dimensional structure of a PL20 enzyme.

2. Materials and methods

2.1. Protein preparation and crystallography

Native TrGL protein was expressed in *Pichia pastoris* and purified as described previously [10]. Selenomethionine-labeled TrGL was expressed in the same transformant cultivated in a Buffered Minimal Medium containing 1% methanol, supplemented with 0.1 mg/mL L-selenomethionine, 0.09 mg/mL L-isoleucine, 0.09 mg/mL L-lysine and 0.6 mg/mL L-threonine as described previously [11]. The filtered culture supernatant was purified by chromatography using Phenyl-Toyopearl and SuperQ-Toyopearl columns (Tosoh). Crystals of native and selenomethionine-labeled TrGL were prepared by the hanging-drop vapor diffusion method at 25 °C by mixing 1.5 μL of protein solution (5.0 mg/mL TrGL in 5.0 mM $CaCl_2$ solution) with 1.5 μL of reservoir solution containing 20% (w/v) PEG3350 and 0.2 M ammonium citrate buffer (pH 5.0). The crystals were transferred to reservoir solutions containing 10–20% (w/v) 2-methyl-2,4-pentanediol and then flash-cooled in a stream of cold nitrogen gas at 100 K. The X-ray diffraction data sets were collected using beamlines at the Photon Factory (Tsukuba, Japan). The data sets were processed and scaled using HKL2000 [12]. SOLVE/RESOLVE [13,14] was used for site detection of selenium, phase calculation and density modification, and automated model building. Manual model rebuilding and refinement were achieved using Coot [15] and Refmac5 [16]. Data collection and refinement statistics are shown in Table 1. Figures were prepared using PyMol (DeLano Scientific). The atomic coordinates and structure factors have been deposited in the Protein Data Bank under the accession code 2ZZJ.

Table 1
Data collection and refinement statistics.

Data set	Native	Selenomethionine		
		Peak	Edge	Remote
A. Data collection				
Beamline	NW12A		BL17A	
Wavelength (Å)	1.000	0.97877	0.97926	0.96403
Space group	$P2_12_12_1$		$P2_12_12_1$	
Cell dimensions				
a (Å)	36.3		36.2	
b (Å)	62.3		62.1	
c (Å)	129.1		128.3	
Resolution (Å)[a]	50–1.8 (1.86–1.80)		50–2.2 (2.28–2.20)	
Total reflections	321020	371020	370774	372089
Unique reflections	27647	27944	28245	27328
Completeness (%)[a]	98.5 (96.9)	99.5 (96.0)	99.0 (92.4)	95.7 (70.8)
Average I/σ (I)[a]	30.8 (4.0)	30.1 (6.1)	28.4 (5.3)	21.8 (3.2)
R_{sym} (%)[a]	6.7 (36.3)	6.6 (16.2)	6.8 (16.6)	7.3 (17.9)
B. Refinement				
Resolution (Å)	34.9–1.80			
R_{work}/R_{free} (%)	18.4/22.3			
Number of reflections	26237			
Number of atoms	2266			
Root mean square deviation from ideal values				
Bond lengths (Å)	0.015			
Bond angles (°)	1.402			
Average B-factor (Å²)				
Protein	21.8			
Calcium ion	17.5			
Citrate	41.9			
Water	37.0			
Ramachandran plot (%)				
Favored	97.0			
Allowed	3.0			
Disallowed	0.0			

[a] Values in parentheses are for the highest resolution shell.

3. Results and discussion

3.1. Overall structure

The crystal structure of TrGL was solved by the multi-wavelength anomalous dispersion method, and the native TrGL structure was determined at 1.8 Å resolution. The TrGL crystal contained one molecule in the asymmetric unit, and the final model contained all the mature protein ranging from Thr1 to Ala238, a calcium ion (Supplementary Fig. S1), a citrate, and 316 water molecules. The TrGL structure has a typical β-jelly roll fold and consists of two antiparallel β-sheets (strands A1–A9 and B1–B7) and two short α-helices (H1 and H2) (Fig. 1 and Supplementary Fig. S2). Sheet B forms a deep cleft, indicating that substrate binding and catalytic reactions occur in the cleft. A disulfide bridge between Cys101 and Cys133 is located in the loops connecting the strands of sheet B. The calcium ion is located far from the cleft, suggesting that it does not contribute to the activity but to the stability of this enzyme.

A database search using the Dali server [17] revealed that TrGL shows high structural similarity to *endo*-1,3-1,4-β-D-glucan 4-glucanohydrolases belonging to glycoside hydrolase family 16. Engineered H(A16-M) enzyme (PDB code 1U0A; *Z* score = 15.5) shows the highest similarity, followed by BGLL from *Bacillus licheniformis* (PDB code 1GBG; *Z* score = 15.1). PL7 alginate lyases, such as A1–II′ from *Sphingomonas* sp. A1 (PDB code 2CWS; *Z* score = 15.0) and PA1167 from *Pseudomonas aeruginosa* PAO1 (PDB code 1VAV; *Z* score = 14.9), exhibit the highest structural similarity within the PL class. PL18 alginate lyase from *Alteromonas* sp. also shows a significant structural similarity (PDB code 1J1T, *Z* score = 14.0). Therefore, PL20 is the third example of a PL family with a β-jelly roll fold.

3.2. Possible catalytic residues

Within the cleft of TrGL, there are positively charged patches formed by arginine residues (Supplementary Fig. S3), which appear to bind the uronate moieties of the substrate. PL20 is a small and highly conserved family; 43 out of about 250 residues are completely conserved among all of the currently available 11 PL20 family members, which are mainly from eukaryotic microbes (Supplementary Fig. S2). The conserved residues are spread over the entire TrGL molecule, but some of them are concentrated at the central part of the cleft wall (Supplementary Fig. S3). Fig. 2A shows the residues in the cleft colored by the degree of conservation. In particular, there are several completely conserved residues on the lower lid of the cleft formed by the helix H1 and β-strand B2.

The catalytic reaction of PLs requires at least two of the following catalytic components: a neutralizer of negative charge on the C6 carboxylate anion and a general base that abstracts the C5 proton at subsite +1. In addition, a general acid that donates a proton to the leaving glycosidic bond oxygen atom is thought to facilitate the reaction in some cases. In Ca^{2+}-dependent enzymes in PL1, 9, and 10, two Ca^{2+} ions held by two Asp residues play a critical role in the charge neutralization of the carboxylate [18–20]. TrGL is also a Ca^{2+}-dependent enzyme [10]. In the crystal structure of TrGL, however, we could not find any Ca^{2+} ions in the cleft. In case of PL1 pectate lyase, the Ca^{2+} ions weakly or hardly bind to the protein in the absence of the substrate carboxyl group [18]. Glu55 may be involved in Ca^{2+} binding of TrGL, since it is the sole acidic residue among the completely conserved residues in the cleft (Fig. 2A).

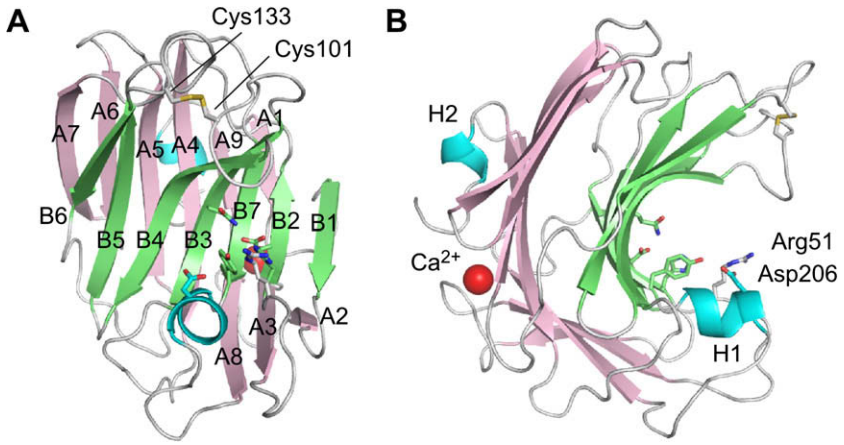

Fig. 1. Overall structure of TrGL. (A) Front and (B) side view of the ribbon representation. The Ca^{2+} ion is shown as a red sphere.

Various amino acid side chains act as the catalytic base in PLs. For example, the catalytic base is Arg in PL1 and 10 [19], Lys in PL9 [20], Tyr in PL5 and 8 [21,22], and His in PL7 [23]. Tyr residue is suggested to be the catalytic acid in PL5 [21], PL8 [22], and PL7 [23], whereas there is no clear catalytic acid in PL1, 9, and 10 [19,20]. The catalytic reaction of PL1, 9, and 10 is thought to proceed through the E1cb or E2 mechanism, and thus, elimination of the leaving group is unlikely to be the rate-limiting step. Among the completely conserved residues in the cleft of TrGL, candidates for the general acid and base are Arg51, His53, Glu55, Tyr200, and Asp206 (Fig. 2A), but the side chains of Arg51 and Asp206 are located at the lid of the cleft (Fig. 1B).

Interestingly, when the structures of two β-jelly roll PL enzymes, TrGL and PL7 A1-II' alginate lyase, are aligned using the secondary structure elements, conserved residues of TrGL clearly overlap with the catalytic residues of A1–II′ (Fig. 2B). The charge neutralizer and the catalytic acid in A1–II′ are Gln189 and Tyr284, respectively [23]. In TrGL, Gln91 and Tyr200 are located at the same positions as Gln189 and Tyr284 in A1–II′, indicating that they play similar roles in the catalysis with those of A1–II′. Moreover, Gln91 residue forms a direct hydrogen bond with Glu55 (Fig. 2A). Therefore, it is suggested that neutralization of the charge on the C6 carboxylate is concomitantly achieved by Gln91 and catalytic Ca^{2+} held by Glu55. The catalytic base of A1–II′ is His191 [23]. In the TrGL structure, Ile93 is located at the corresponding position, but this residue cannot act as the base catalyst. Since A1–II′ can cleave both poly-α-L-guluronate and poly-β-D-mannuronate, it catalyzes both *anti*- and *syn*-elimination reactions. His191 is the catalytic base in the *anti*-elimination reaction because it is located near the C5 atom of a-L-guluronate bound at subsite +1 in the model complex structure of wild-type A1–II′ and the substrate [23]. Although the catalytic base of A1–II′ in the *syn*-elimination reaction is unclear, Tyr284 possibly plays a dual role of catalytic base and acid as in the case of PL5 alginate lyase A1–III [21] and PL8 chondroitin AC lyase [22]. Since TrGL catalyzes the *syn*-elimination of the β-(1→4)-glucuronate bond, Tyr200 likely plays a dual role of catalytic base and acid. In the A1–II′ structure, a conserved Arg146 residue is located near the catalytic acid, Tyr284. Arg146 in A1–II′ is thought to modulate the pK_a of Tyr284 hydroxyl group [23]. A completely conserved His53 residue in TrGL, which is located at the position corresponding to Arg146 in A1–II′, may help the catalytic role of Tyr200, or may itself act as the catalytic base and/or acid. In order to clarify the substrate recognition mechanism and the identity of the catalytic residues of TrGL, further studies, such as mutational analysis and determination of the complex structures with substrates or analogues, will be required.

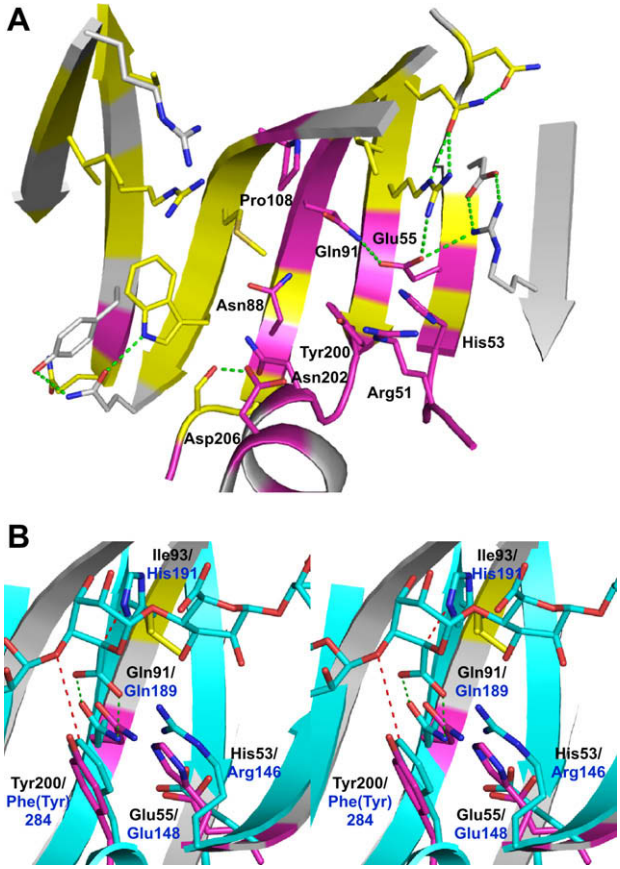

Fig. 2. Residues in the cleft of the β-jelly roll fold. (A) Residues in the cleft of TrGL. Carbon atoms are colored by residue conservation; completely and partially conserved residues are shown in magenta and yellow, respectively. Completely conserved residues are labeled. Hydrogen bonds are shown by green dotted lines. (B) The structure of TrGL is superimposed with that of PL7 alginate lyase A1–II′ (cyan) using the overall secondary elements. The A1–II′ structure is a composite of the Y284F mutant complexed with trisaccharide (PDB code 2ZAC, protein) and the H191N/Y284F mutant complexed with tetrasaccharide (PDB code 2ZAA, ligand). The proposed interactions for the catalytic base and acid reactions of A1–II′ are indicated by red dotted lines.

Acknowledgments

We thank the staff of the Photon Factory for the X-ray data collection. This work was supported by Grant-in-Aids for Scientific Research to N.K. (No. 20-7128) from the Japan Society for the Promotion of Science (JSPS) and a grant for development of biomass utilization technologies for revitalizing rural areas to M.S. from the Japanese Ministry of Agriculture, Forestry and Fisheries.

Appendix A. Supplementary data

Supplementary data associated with this article can be found, in the online version, at doi:10.1016/j.febslet.2009.03.034.

References

[1] Cantarel, B.L., Coutinho, P.M., Rancurel, C., Bernard, T., Lombard, V. and Henrissat, B. (2008) The Carbohydrate-Active enZymes database (CAZy): an expert resource for Glycogenomics. Nucleic Acids Res. 37, D233–D238.
[2] Aono, R. (1990) The poly-alpha- and -beta-1, 4-glucuronic acid moiety of teichuronopeptide from the cell wall of the alkalophilic *Bacillus* strain C-125. Biochem. J. 270, 363–367.
[3] Tsuchihashi, H., Yadomae, T. and Miyazaki, T. (1983) Structural analysis of the cell-wall D-glucuronans from the fungi *Absidia cylindrospora*, *Mucor mucedo*, and *Rhizopus nigricans*. Carbohydr. Res. 111, 330–335.
[4] Bobin-Dubigeon, C., Lahaye, M., Guillon, F., Barry, J.L. and Gallant, D.J. (1997) Factors limiting the biodegradation of *Ulva* sp. cell-wall polysaccharides. J. Sci. Food Agric. 75, 341–351.
[5] Sugimoto, I., Onimatsu, H., Fujie, M., Usami, S. and Yamada, T. (2004) VAL-1, a novel polysaccharide lyase encoded by chlorovirus CVK2. FEBS Lett. 559, 51–56.
[6] Da Costa, A., Michaud, P., Petit, E., Heyraud, A., Colin-Morel, P., Courtois, B. and Courtois, J. (2001) Purification and properties of a glucuronan lyase from *Sinorhizobium meliloti* M5N1CS (NCIMB 40472). Appl. Environ. Microbiol. 67, 5197–5203.
[7] Delattre, C., Michaud, P., Keller, C., Elboutachfaiti, R., Beven, L., Courtois, B. and Courtois, J. (2006) Purification and characterization of a novel glucuronan lyase from *Trichoderma* sp. GL2. Appl. Microbiol. Biotechnol. 70, 437–443.
[8] Konno, N., Habu, I., Maeda, I., Azuma, N. and Isogai, A. (2006) Cellouronate (beta-1,4-linked polyglucuronate) lyase from *Brevundimonas* sp. SH203: purification and characterization. Carbohydr. Polym. 64, 589–596.
[9] Konno, N., Habu, I., Iihashi, N. and Isogai, A. (2008) Purification and characterization of exo-type cellouronate lyase. Cellulose 15, 453–463.
[10] Konno, N., Igarashi, K., Habu, N., Samejima, M. and Isogai, A. (2009) Cloning of the *Trichoderma reesei* cDNA encoding a glucuronan lyase belonging to a novel polysaccharide lyase family. Appl. Environ. Microbiol. 75, 101–107.
[11] Ishida, T., Fushinobu, S., Kawai, R., Kitaoka, M., Igarashi, K. and Samejima, M. (in press). Crystal structure of glycoside hydrolase family 55 beta-1,3-glucanase from the basidiomycete *Phanerochaete chrysosporium*. J. Biol. Chem, doi:10.1074/jbc.M808122200.
[12] Otwinowski, Z. and Minor, W. (1997) Processing of X-ray diffraction data collected in oscillation mode. Methods Enzymol. 276, 307–326.
[13] Terwilliger, T.C. and Berendzen, J. (1999) Automated MAD and MIR structure solution. Acta Crystallogr. D Biol. Crystallogr. 55, 849–861.
[14] Terwilliger, T.C. (2000) Maximum-likelihood density modification. Acta Crystallogr. D Biol. Crystallogr. 56, 965–972.
[15] Emsley, P. and Cowtan, K. (2004) Coot: model-building tools for molecular graphics. Acta Crystallogr. D Biol. Crystallogr. 60, 2126–2132.
[16] Murshudov, G.N., Vagin, A.A. and Dodson, E.J. (1997) Refinement of macromolecular structures by the maximum-likelihood method. Acta Crystallogr. D Biol. Crystallogr. 53, 240–255.
[17] Holm, L. and Sander, C. (1995) Dali: a network tool for protein structure comparison. Trends Biochem. Sci. 20, 478–480.
[18] Herron, S.R., Benen, J.A., Scavetta, R.D., Visser, J. and Jurnak, F. (2000) Structure and function of pectic enzymes: virulence factors of plant pathogens. Proc. Natl. Acad. Sci. USA 97, 8762–8769.
[19] Charnock, S.J., Brown, I.E., Turkenburg, J.P., Black, G.W. and Davies, G.J. (2002) Convergent evolution sheds light on the anti-beta-elimination mechanism common to family 1 and 10 polysaccharide lyases. Proc. Natl. Acad. Sci. USA 99, 12067–12072.
[20] Jenkins, J., Shevchik, V.E., Hugouvieux-Cotte-Pattat, N. and Pickersgill, R.W. (2004) The crystal structure of pectate lyase Pel9A from *Erwinia chrysanthemi*. J. Biol. Chem. 279, 9139–9145.
[21] Yoon, H.J., Hashimoto, W., Miyake, O., Murata, K. and Mikami, B. (2001) Crystal structure of alginate lyase A1–III complexed with trisaccharide product at 2.0 A resolution. J. Mol. Biol. 307, 9–16.
[22] Lunin, V.V., Li, Y., Linhardt, R.J., Miyazono, H., Kyogashima, M., Kaneko, T., Bell, A.W. and Cygler, M. (2004) High-resolution crystal structure of *Arthrobacter aurescens* chondroitin AC lyase: an enzyme-substrate complex defines the catalytic mechanism. J. Mol. Biol. 337, 367–386.
[23] Ogura, K., Yamasaki, M., Mikami, B., Hashimoto, W. and Murata, K. (2008) Substrate recognition by family 7 alginate lyase from *Sphingomonas* sp. A1. J. Mol. Biol. 380, 373–385.